COMMUNICATION

Journal of Materials Chemistry
www.rsc.org/materials

Density control of single-walled carbon nanotubes using patterned iron nanoparticle catalysts derived from phase-separated thin films of a polyferrocene block copolymer†

Sarah Lastella,[a] Yung Joon Jung,[a] Hoichang Yang,[a] Robert Vajtai,[a] Pulickel M. Ajayan,*[a] Chang Y. Ryu,*[a] David A. Rider[b] and Ian Manners*[b]

[a]*Rensselaer Nanotechnology Center, Rensselaer Polytechnic Institute, Troy, NY 12180, USA. E-mail: ajayan@rpi.edu; E-mail: ryuc@rpi.edu; Fax: (518) 276-4887; Tel: (518) 276-2060*

[b]*Department of Chemistry, University of Toronto, Toronto, Ontario, M5S 3H6, Canada. E-mail: imanners@chem.utoronto.ca; Fax: (416) 978-6157; Tel: (416) 978-6157*

Received 12th March 2004, Accepted 28th April 2004
First published as an Advance Article on the web 19th May 2004

DOI: 10.1039/b403831b

Single-walled carbon nanotube (SWNT) density and bundle size has been controlled by a simple one step CVD growth process using a polyferrocenylsilane block copolymer as the pre-organized catalyst source.

Single-walled carbon nanotubes (SWNTs) are becoming the focus of nano-device fabrication[1] because of their high aspect ratio, strength, and electronic properties. However, one of the main stumbling blocks in this area is facile formation of a uniformly dispersed network of tube junctions on the nano-scale while maintaining a clean surface. Nanotubes spin cast onto a surface will always agglomerate due to poor interactions with solvents unless functionalized.[2] It is therefore necessary to grow rather than deposit nanotubes on a substrate surface in order to achieve uniform dispersities. One SWNT growth technique is to deposit the catalyst onto a substrate with electron beam lithography techniques, where upon heating, the catalyst forms spheres on the surface.[3] This does not allow for precise control of catalyst size or spacing. Another approach is to organize nanoparticles using porous substrates or templates, such as the ferritin protein containing holes in which Liu and coworkers have trapped iron catalysts.[4] Although the nanoparticle diameters can be controlled fairly well, a more simplified approach is preferred. Soft lithography using an elastomer stamp and a poly(styrene-*r*-vinylferrocene) random copolymer followed by CVD demonstrated micropatterned NT growth.[5] Here, we report a simple clean process in which SWNT growth density and bundle diameter can be controlled. A pyrolyzed diblock copolymer thin film containing both an inorganic (iron containing) and organic component has been used to catalyze SWNT growth during chemical vapor deposition (CVD). The organometallic block is uniformly spaced throughout the polymer film as a result of natural block copolymer morphological ordering. Upon heating, the inorganic constituent transforms into iron nanoparticles as the remainder of the polymer matrix is vaporized. It is possible to control the size and dispersion of nanoparticles on the surface by varying the film thickness, and in turn we can control the nanotube density and bundle diameters. The simplicity of this process and the ease of parameter control make it highly promising for SWNT device applications.

Polyferrocenylsilane block copolymers are readily available *via* living anionic ring-opening polymerization techniques.[6] Thin films phase separate into organometallic nanodomains which are able to serve as precursors to iron-rich ceramic nanodomain replicas above 500 °C.[6–10] In this work we have used an amorphous asymmetric PS-*b*-PFEMS (PS = polystyrene, PFEMS = polyferrocenylethylmethylsilane) block copolymer[7] which forms spheres of PFEMS in a matrix of PS.†

Scheme 1 illustrates how the PS-*b*-PFEMS block copolymer chains organize relative to one another in order to minimize interaction energies. The PFEMS regions form spheres which are uniformly spaced on the surface by the PS chain segments. With a PFEMS volume ratio of 12% and a number average molecular weight of 63.7 kg mol^{-1}, the spheres are approximately 20 nm in diameter with a separation distance of 45 nm. It can be estimated that approximately 12400 iron atoms are present in each spherical region of PFEMS. During the heating process, the ferrocene groups in the PFEMS domains convert into iron nanoparticles.[10] XPS was used to determine the composition of the silica surface after CVD to approximate the iron density. Table 1 shows iron made up only 0.6% of the surface composition, corresponding to the largely spaced nanoparticles and nanotubes. The AFM image in Scheme 1 illustrates the nanoparticle distribution on the substrate surface. The large amount of oxide and silicon in the XPS spectrum is due to the plasma grown oxide and substrate.

Typical SWNT growth from spin cast pyrolyzed films of PS-*b*-PFEMS is shown in Fig. 1. Note the tubes are uniformly dispersed as a result of the block copolymer organization on the substrate surface prior to heating. The surface is also very clean because the hydrocarbons are easily vaporized during the heating process, leaving behind mainly iron and silicon compounds. This is also evidenced by Raman spectroscopy† which gave no disordered graphene peak between 1320 and 1340 cm^{-1}, indicating that the nanotubes are relatively free of amorphous carbon and defects.[11]

In Fig. 2a, the Raman peaks at ~1570 cm^{-1} and ~1590 cm^{-1} represent ordered graphite signals (tangential mode) indicative of carbon nanotubes. The diameter dependent peaks in the region of 100 to 400 cm^{-1} represent the radial breathing mode[12] (RBM), as seen in Fig. 2b. The diameters are found by equation (1):[13–15]

$$d = (223.75\ \text{cm}^{-1}/\text{nm})/(\text{peak} - 14) \quad (1)$$

The diameter (d) represented in nm is inversely proportional to the RBM peak in cm^{-1} by a factor of 223.75. This constant is generally accepted and is derived from experimental results. When the nanotubes are found in bundles rather than in

† Electronic supplementary information (ESI) available: synthesis of PS-*b*-PFEMS, SWNT growth and characterization. See http://www.rsc.org/suppdata/jm/b4/b403831b/

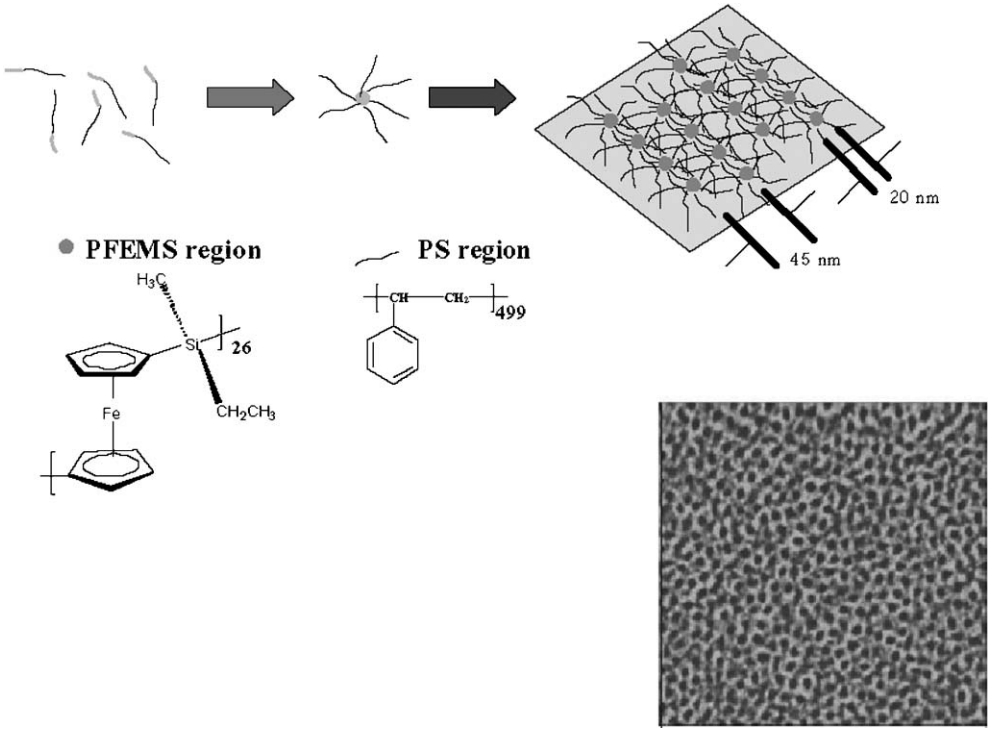

Scheme 1 Self-assembly of PS-*b*-PFEMS and AFM height image (1 μm^2) of spin cast film. Dark regions are PFEMS while lighter regions are PS.

isolated environments, they experience an added pressure which shifts the peak approximately 14 cm^{-1}. In this case, the diameters are calculated from the above equation, since the diameters seen in AFM (averaging around 5 nm) are too large for individual SWNT dimensions.[4] The diameters found with the SWNT RBM peak range from 0.66 to 1.1 nm.

The PS-*b*-PFEMS thin films were determined to be *ca.* 25, 40, and 100 nm in thickness by AFM on scratched samples when polymer solutions of 0.5 wt%, 1.0 wt%, and 2.5 wt% were spin cast onto silica substrates, respectively. It was found that with polymer solution concentrations of 0.1 wt% and below, nanotube growth was inconsistent, most likely due to dewetting of the thin film. At higher solution concentrations (0.5 wt% and above), nanotubes grew consistently because the block copolymer dimensions (PFEMS spherical domains are *ca.* 20 nm) were equal to or lower than the film thickness. It should be noted that nanotube growth did not depend on substrate type in this study (silica *vs.* silicon).

With these three film thicknesses of 25, 40 and 100 nm, two trends were realized. As film thickness increased, nanotube bundle diameters increased while growth density decreased. The nanotube diameters grown from the 0.5 wt% thin films averaged between 2 and 5 nm, as illustrated in Fig. 3. As film thickness increased to 40 and then 100 nm, the average diameters grew to ranges of 5 to 9 nm and 10 to 20 nm, respectively. Fig. 3c shows a 2.5 wt% CVD grown film where the bundle is *ca.* 17 nm in diameter.

Fig. 3 also gives evidence of density control through film thickness. Although the growth density is fairly similar between the 0.5 wt% and 1.0 wt% spin cast samples, it can be seen that a large film thickness will eventually inhibit nanotube growth, as in the 2.5 wt% sample. To further illustrate this thickness effect, two different film thicknesses were created on one sample *via* soft lithography.[5] A polydimethylsiloxane (PDMS) stamp containing various line and dot patterns was pressed onto a silicon substrate wet with 0.5 wt% block copolymer

Table 1 X-Ray photoelectron spectroscopy of substrates after thin film preparation and SWNT growth

Element (Electron Shell)	Atomic Percent
C (1s)	27.5
O (1s)	47.5
Si (2p)	24.4
Fe (2p)	0.6

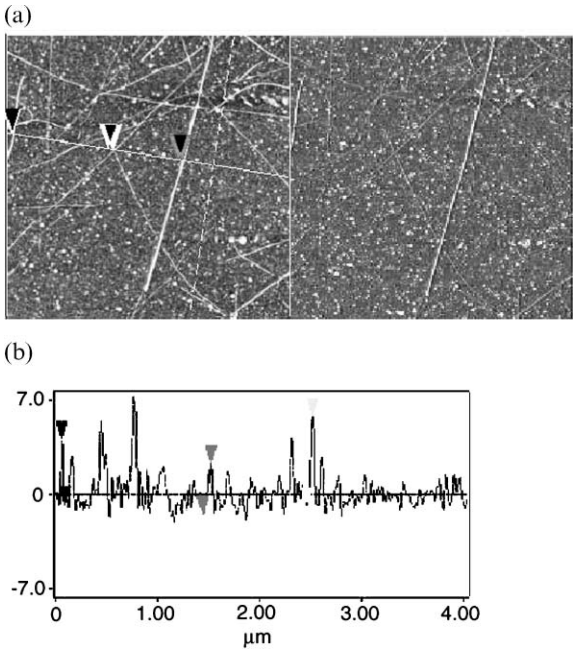

Fig. 1 SWNT bundles from Fe nanoparticles on silica substrate. (a) AFM height image (left) and phase image (right) (16 μm^2). (b) Height profile of solid white line seen in (a): dark markers (left) show a single NT bundle height of 4.8 nm; gray markers (middle) show two crossed NT bundles with a combined height of 3.8 nm; light markers (right) show a larger nanotube bundle with a diameter of 6.6 nm.

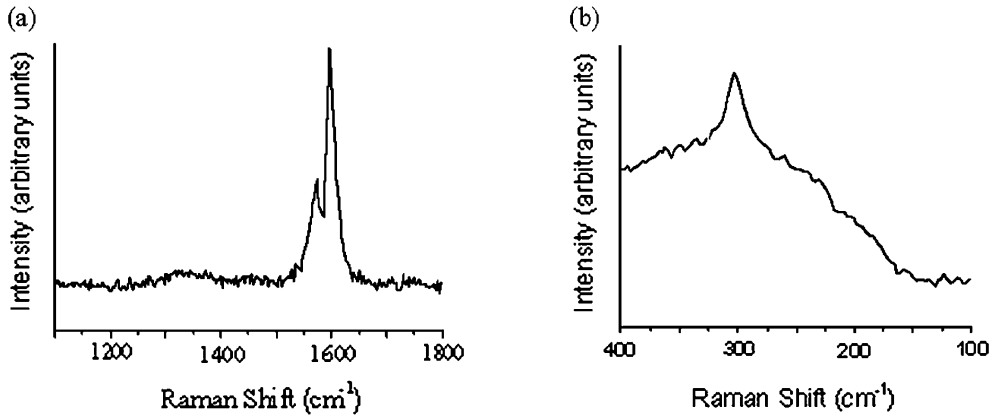

Fig. 2 Raman spectra (a) tangential mode showing G and D bands at 1590 and 1340 cm^{-1} respectively; (b) radial breathing mode.

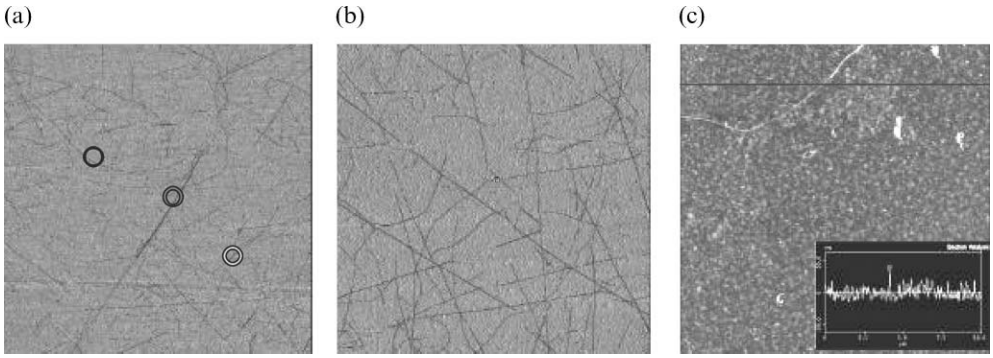

Fig. 3 AFM phase images (a, b) and height image (c) (100 μm^2) depicting CNT growth from various PS-*b*-PFEMS spin cast solutions: (a) 25 nm film from 0.5 wt% solution; dark ring marks bundle diameter of 2.3 nm; grey ring marks 4.5 nm bundle; light ring marks 3.0 nm bundle. (b) 40 nm film from 1.0 wt% solution; average bundle diameters of 5.0 to 9.0 nm. (c) *Ca.* 100 nm film from 2.5 wt% solution; bundle diameter of 17.7 nm as indicated by height profile (inset) from scan line.

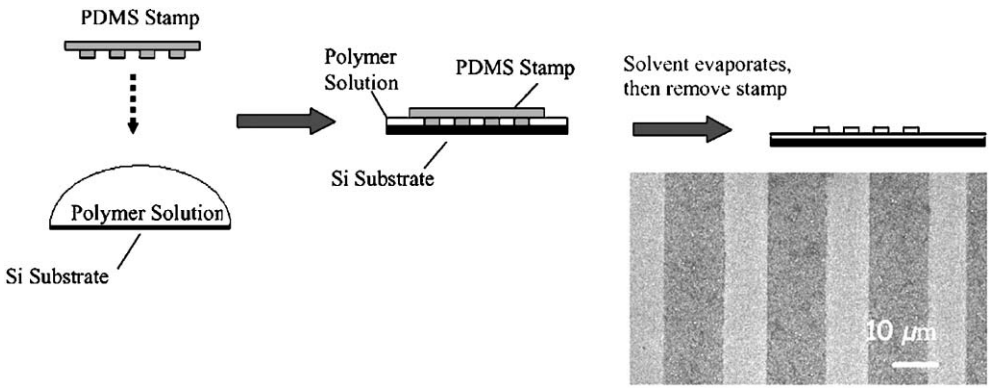

Scheme 2 Process for depositing PS-*b*-PFEMS at different film thicknesses *via* a PDMS stamp and SEM image of the resulting film. Lighter areas are *ca.* 50 nm and darker areas are *ca.* 200–300 nm thick.

solution. When the toluene had completely evaporated from the substrate, the stamp was removed to reveal both thick (~200–300 nm) and thin (~50 nm) PS-*b*-PFEMS regions. Scheme 2 illustrates this process, showing the final SEM image of the pattern still visible on the substrate after the CVD process. Fig. 4 illustrates that in the very thick polymer regions, few to no SWNTs grow, while a high density of nanotubes grow in the thin polymer areas. Therefore, a PS-*b*-PFEMS film over 100 nm in thickness contains an abundance of iron domains, which upon heating, agglomerate into larger nanoparticles and prevent SWNT growth. This also accounts for the fact that the nanotube bundles will increase with catalyst size, as shown previously in Fig. 3.

We have demonstrated that SWNT growth density was easily and reproducibly controlled by varying the film thickness of a self-assembled PS-*b*-PFEMS block copolymer. In this way, the amount of iron on the substrate surface could be tuned to produce smaller catalyst particles,[16] which in turn decrease nanotube bundle diameters while simultaneously increasing growth density. This process produces clean, uniformly dispersed SWNTs, as evidenced from Raman spectroscopy and AFM. The simplicity of this growth process, coupled with the ideal tube purity and dispersion, the possibility for controlling catalyst particle size and hence SWNT dimensions by adjusting the block ratio and overall molecular weight of PS-*b*-PFEMS, and the ability to use soft-lithographic patterning methods make this scheme a highly promising method for the creation of nanoelectronic devices.

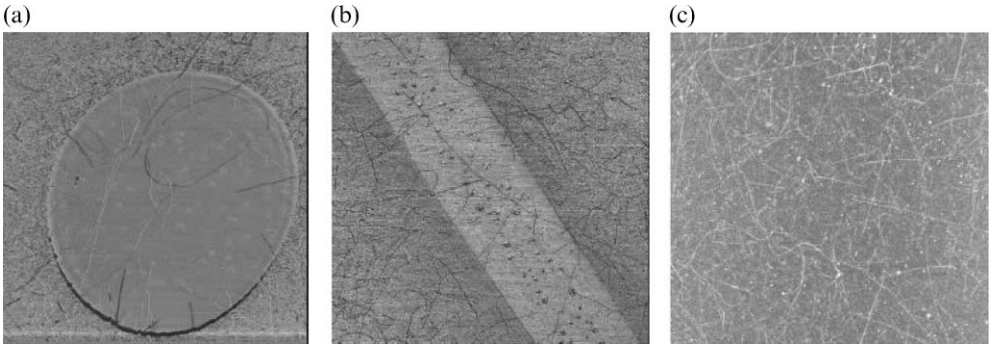

Fig. 4 PDMS stamped silicon substrates with 0.5 wt% PS-*b*-PFEMS solutions after CVD: (a) 100 μm^2 AFM phase image; (b) 400 μm^2 AFM phase image. The thick polymer regions (>200 nm prior to CVD) are seen as a circle in (a), and bar in (b) as a result of the patterned stamp. Thin regions outside these shapes have high densities of SWNTs. (c) 100 μm^2 AFM height image of thin polymer region (darker) outside the thick polymer line (lighter) further illustrating the high density nanotube growth from an optimum polymer film thickness.

Acknowledgements

D.A.R. and I.M. thank the Natural Science and Engineering Research Council of Canada (NSERC) for financial support of this work. We also acknowledge University of Toronto Open Fellowships for D.A.R. In addition, S.L. and C.Y.R. thank GAANN for fellowships. Y.J.J., H.Y., R.V. and P.M.A. thank supports from NSEC and Focus Center-New York at Rensselaer.

Notes and references

1 M. S. Dresselhaus, G. Dresselhaus and P. Avouris, *Carbon Nanotubes: Synthesis, Structure, Properties, and Applications*, Springer, Berlin, New York, 2001.
2 Y.-P. Sun, K. Fu, Y. Lin and W. Huang, *Acc. Chem. Res.*, 2002, **35**, 1096.
3 Y. J. Jung, B. Wei, R. Vajtai, P. M. Ajayan, Y. Homma, K. Prabhakaran and T. Ogino, *Nano Lett.*, 2003, **3**, 561.
4 M. Su, Y. Li, B. Maynor, A. Buldum, J. P. Lu and J. Liu, *J. Phys. Chem. B*, 2000, **104**, 6505.
5 E. Lahiff, C. Y. Ryu, S. Curran, A. I. Minett, W. J. Blau and P. M. Ajayan, *Nano Lett.*, 2003, **3**, 1333.
6 Y. Ni, R. Rulkens and I. Manners, *J. Am. Chem. Soc.*, 1996, **118**, 4102.
7 K. Temple, J. A. Massey, Z. Chen, N. Vaidya, A. Berenbaum, M. D. Foster and I. Manners, *J. Inorg. Organomet. Polym.*, 1999, **9**, 189.
8 I. Manners, *Chem. Commun.*, 1999, 857; R. G. H. Lammertink, M. A. Hempenius, E. L. Thomas and G. J. Vancso, *J. Polym. Sci. Polym. Phys.*, 1999, **37**, 1009.
9 I. Manners, *Science*, 2001, **294**, 1664.
10 K. Temple, K. Kulbaba, K. N. Power-Billard, I. Manners, K. A. Leach, T. Xu, T. P. Russell and C. J. Hawker, *Adv. Mater.*, 2003, **15**, 297.
11 A. M. Rao, J. Chen, E. Richter, U. Schlecht, P. C. Eklund, R. C. Haddon, U. D. Venkateswaran, Y.-K. Kwon and D. Tománek, *Phys. Rev. Lett.*, 2001, **86**, 3895.
12 For recent work involving the assignment of similar radial breathing modes of single walled carbon nanotubes see: I. L. Li and Z. K. Tang, *Appl. Surf. Sci.*, 2004, **226**, 72; R. Seidel, G. S. Duesberg, E. Unger, A. P. Graham, M. Liebau and F. Kreupl, *J. Phys. Chem. B*, 2004, **108**, 1888.
13 S. Bandow, S. Asaka, Y. Saito, A. M. Rao, L. Grigorian, E. Richter and P. C. Eklund, *Phys. Rev. Lett.*, 1998, **80**, 3779.
14 B. Wei, R. Vajtai, Y. Y. Choi, P. M. Ajayan, H. Zhu, C. Xu and D. Wu, *Nano Lett.*, 2002, **2**, 1105.
15 L. Sangaletti, S. Pagliara, F. Parmigiani, P. Galinetto, R. Larciprete, S. Lizzit and A. Goldoni, *Eur. Phys. J. B*, 2003, **31**, 203.
16 During the thermal treatment the PS is lost and the ceramic residue consists of PFS-derived Fe nanoparticles (see ref. 10). As the film thickness increases, larger amounts of Fe would be expected to be left on the surface.